

Palladium-Doped Zinc Oxide Nanomaterial For Liquefied Petroleum Gas Detection.

Yogita Patil¹, R. B. Pedhekar², F. C. Raghuvanshi³

¹Government College of Engineering, Jalgaon 425002, India

²M. J. Fule Commerce, Science & V. Raut Arts College, Bhatkuli Dist. Amravati 444602, India.

³Dean, Faculty of Science & Technology, Sant Gadge Baba Amravati University, Amravati 444602, India.

Corresponding Author: Yogita Patil

Abstract: The liquid petroleum gas sensing characteristics of Palladium doped zinc oxide (ZnO) films have been studied. Microwave synthesis method was used for synthesis of zinc oxide and Palladium doped zinc oxide nanomaterial and screen printing technology was used to prepare thick-film sensor element. The thick films were characterized by using X-ray diffractogram, field emission scanning electron microscopy and energy dispersive X-ray analysis. The 3 wt. % Pd doped ZnO thick film show sensitivity to LPG at room temperature and maximum sensitivity at 350 °K temperature with fast response and recovery time.

Keywords: Gas sensor, Palladium, Thick film, ZnO.

Date of Submission: 20-01-2020

Date of Acceptance: 05-02-2020

I. Introduction

Zinc oxide nanomaterial play an important role in applications of electronic devices, in particular for gas sensing. The growth conditions of ZnO nanocrystals affects availability of ZnO crystals in distributed discrete gas sensing devices and the uniformity, size and defects of ZnO nanocrystals are strongly influenced by this condition. Gas sensing and optical properties of ZnO nanomaterial differ from the bulk materials i.e. sensitivity and selectivity are sufficiently high in case of nanomaterial. ZnO nanomaterials possess a large surface atom/bulk atom ratio. This ratio correspondence to a higher sensitivity, thermal stability and compatibility with other nano devices [1- 8]. Hence ZnO nanomaterials are used as a gas sensor. ZnO nanorods resist formation of rust. Because of these properties, ZnO is widely used in chemical and humidity sensing devices. Metal oxides cannot easily differentiate between different types of gases, but by adding certain noble metals as dopants can enhance the gas sensing performance [9 -15]. The optical and electrical properties of ZnO can be enhanced by adding Noble dopants in ZnO which increase the sensitive performance. Palladium metal is used as an impurity in ZnO because of its special electronic configuration, i.e., 4d. Due to the sensitivity of the palladium ions with deep holes on singly ionized oxygen interstitials, Zn anti-site vacancies, and oxygen vacancies, it is of interest to find out whether Pd incorporated in ZnO significantly improves sensitivity and specificity [16 - 19].

In long term devices and space craft's hydrogen sensors based on Pd are used for detection of hydrogen leaked from fuel cells and proton-exchange membrane to minimized weight and power of sensor. Chemical vapour deposition (CVD), RF sputtering methods to prepare ZnO nanorods or doping of Pd in ZnO are expensive methods [20, 21].

In this work, we report the microwave assisted synthesis of Pd doped ZnO nanomaterial. Pd doped ZnO nanomaterials were synthesized by using simple instruments i. e. microwave and magnetic stirrer. The effect of dopant concentrations on structural properties were studied from X-ray diffraction (XRD) and morphological properties were studied by using scanning electron microscopy (SEM). Synthesized powders were used to fabricate the sensor elements in the form of thick films with a screen printing technique and gas sensing response of prepared thick films were tested for different gases i. e. NH₃, H₂S, CO₂, LPG and Ethanol gas.

II. Experimental

2.1 Synthesis of pure and Pd doped ZnO:

In preparation of pure and Palladium doped ZnO nanomaterial, zinc acetate ((CH₃COO)₂. Zn. 2H₂O) and Palladium chloride (0 wt. %, 1 wt. %, 3wt. % and 6wt. %) were dissolved in 100 ml deionized water and magnetically stirred for 30 minutes. Then 2 M sodium hydroxide (NaOH) solution was prepared and introduced into the zinc acetate solution with continues stirring. The solution was ultrasonicated for 15 minutes and then it was kept in microwave for 15 minutes. The solution was allowed to cool down at room temperature naturally.

After that solution was filtered and precipitate was washed with deionized water and absolute ethanol to remove the excess and contaminated salts. The obtained powder was dried at 343 °K in oven. Fig.1 shows the photographs of Synthesized of Pd-doped ZnO.

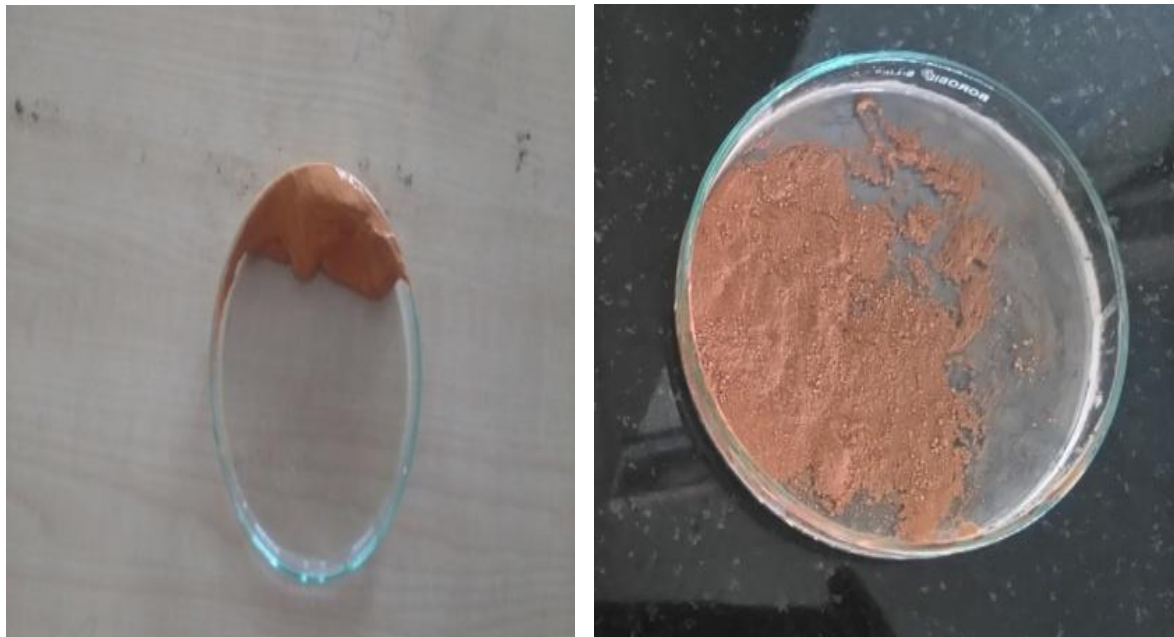


Figure 1: Photographs of Synthesized of Pd-doped ZnO.

2.2 Fabrication of thick films and gas sensing measurements:

For preparation of thick films, thixotropic paste of synthesized material was prepared and ethyl cellulose is used as temporary binder with mixture of organic solvents such as butyl carbitol acetate, butyl cellulose and turpineol. The synthesized materials were mixed with solution of ethyl cellulose and mixture of organic solvents. The ratio of organic to inorganic part was maintained as 20:80 in formation of paste. The binder was used for binding of material with glass substrate. The thick films were prepared by screen printing method. In this method, paste is robbed on the glass substrate by applying uniform pressure. The fabricated thick films were fired at 500 °C for half an hour for removal of organic material.

The electrical contacts were made by using silver electrodes to measure gas sensing properties. For gas sensing measurements, static gas sensing system was used. The gas concentration for experiment was fixed to 1000 ppm and gas sensing response of thick film was noted. The sensor response (S) was defined as the ratio of resistance of sensor element in air (R_a) to that in target gas (R_g) [22].

$$S = R_a / R_g \quad (1)$$

III. Results And Discussion

3.1 Thick film Characterization techniques:

3.1.1 X-ray diffraction analysis:

X-ray diffraction study of pure and Pd doped ZnO thick films were carried out using BRUKER AXSD8 (Germany) advance model X ray diffraction with $\text{CuK}\alpha_1$ ($\lambda=1.54056 \text{ \AA}$) radiation in the 2θ range 20° - 80° . The scanning speed of the specimen was maintained $0.5^\circ/\text{min}$.

Fig.2 shows the XRD spectra of (a) Pure ZnO, (b) 1wt.% Pd doped ZnO, (c) 3 wt.% Pd doped ZnO, (d) 6 wt. % Pd doped ZnO thick films. The peaks of pure and Pd doped ZnO are obtained at (100), (002), (101), (102), (110), (103), (112) and (201) planes. The peaks assigned to diffraction from various planes correspond to hexagonal Wurtzite structure of ZnO. It is observed that two additional peaks are obtained at 30.68° and 57.95° , which can be associated with PdO [23]. These peaks can be associated with (1 0 0) and (1 1 2) or (2 2 0) PdZn intermetallic compound [24]. The intensities of the peaks obtained at 30.68° and 57.95° , increases with increase in percentage of Pd doping in ZnO. The results show that Pd - doped ZnO sample has a better crystallinity, higher intensity and smaller peak width than those of the pure ZnO. The crystalline sizes of the ZnO and Pd doped ZnO were determined by means of X-ray line –broadening method using Debye–Scherrer's formula [25].

$$D = \frac{0.9 \lambda}{\beta \cos \theta} \quad (2)$$

Where, D is the crystallite size in nanometer, λ is the X-ray radiation (0.154056 nm for $\text{CuK}\alpha$ radiation) wavelength, θ is the Bragg diffraction angle and β is full width at half maxima intensity (FWHM). No diffraction peaks of other compounds were observed in ZnO which indicates that the ZnO nano structures have high crystallinity and purity. The crystallite size for Pure ZnO, 1wt.% Pd doped ZnO, 3 wt.% Pd doped ZnO, and 6 wt. % Pd doped ZnO was found to be 49 nm, 43 nm, 33 nm and 42 nm respectively. Thus, it is observed due to Pd doping, there is decrease in crystallite size.

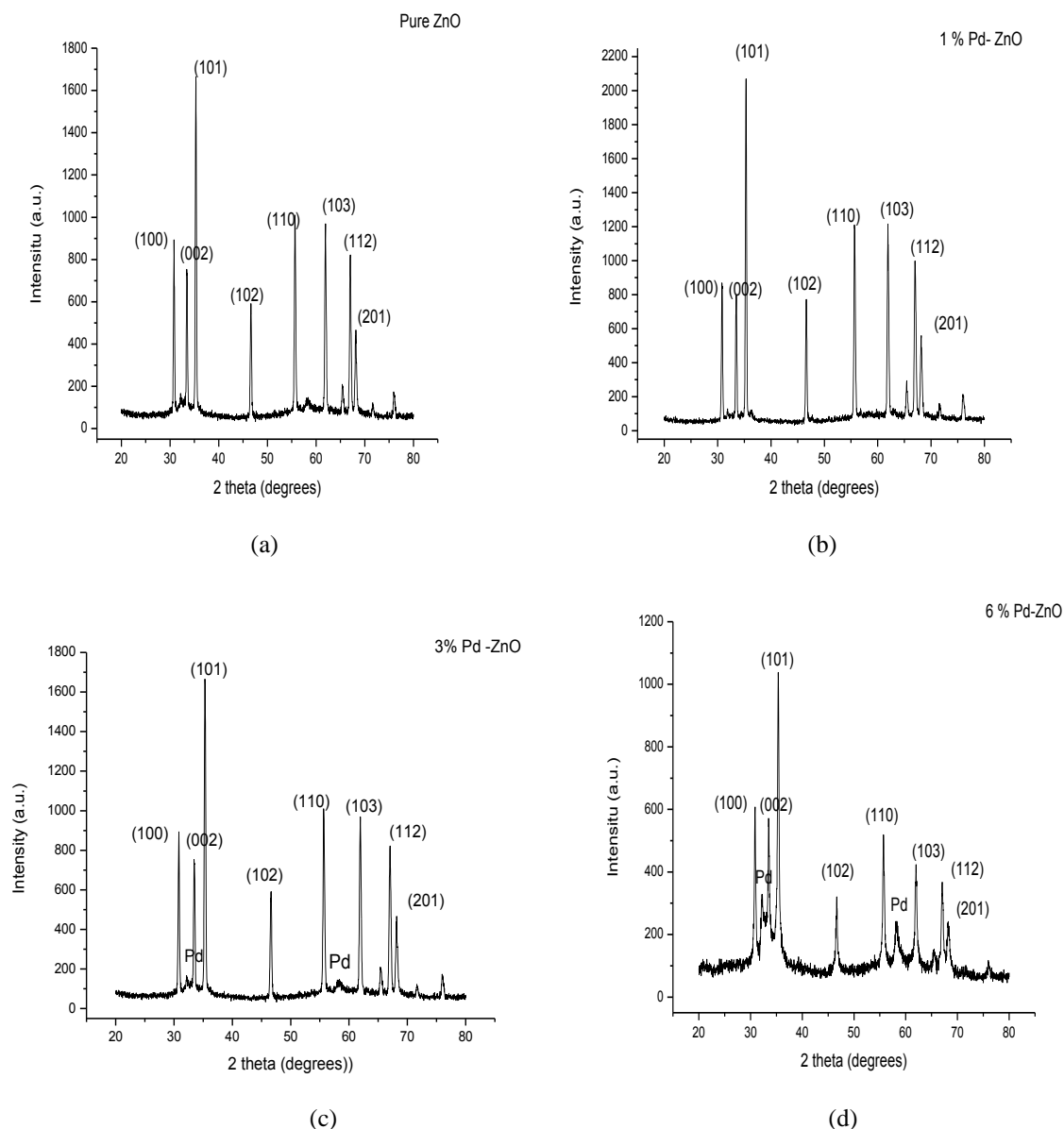
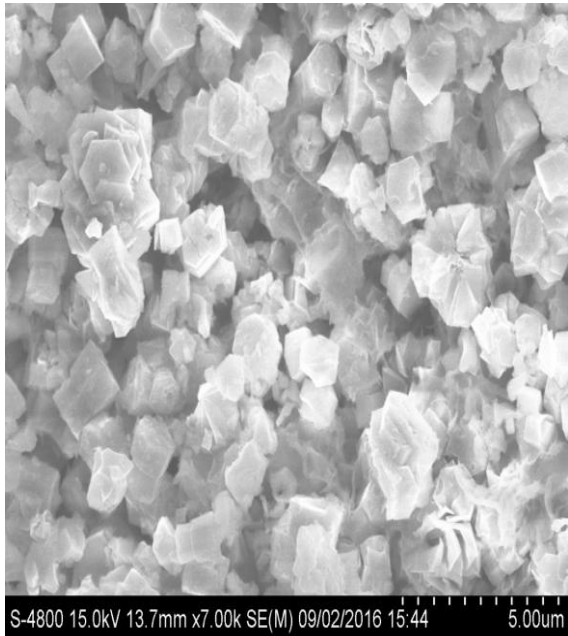


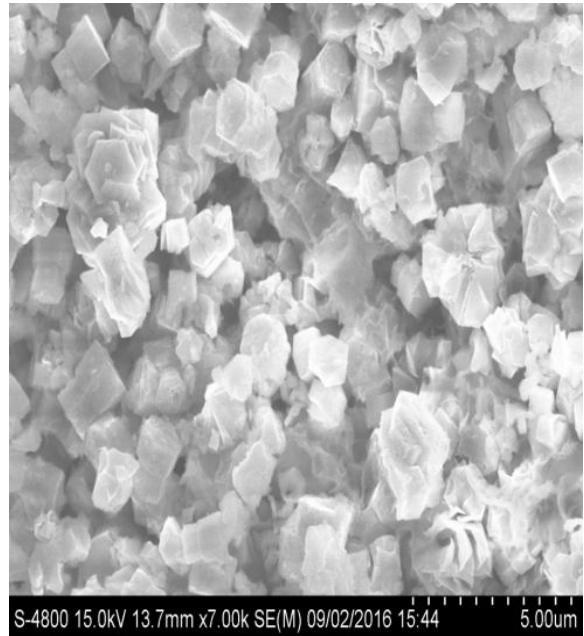
Figure 2: XRD spectra of (a) Pure ZnO, (b) 1 wt.% Pd doped ZnO, (c) 3 wt.% Pd doped ZnO, (d) 6 wt. % Pd doped ZnO thick films.

3.1.2 Field emission scanning electron microscopy (FE-SEM):

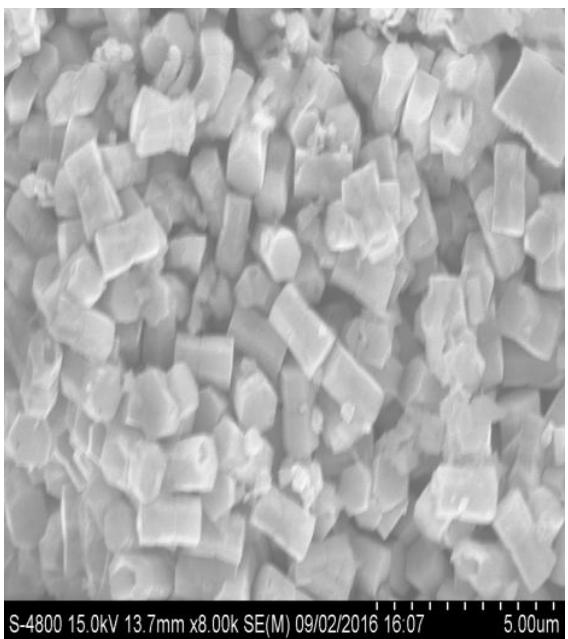
Fig. 3 (a – e) shows the FESEM images of (a) Pure ZnO, (b) 1wt.% Pd doped ZnO, (c) 3 wt.% Pd doped ZnO, (d) 6 wt. % Pd doped ZnO and (e) high resolution image of 3 wt.% Pd doped ZnO. Fig. 2 (a) and (b) shows bulk quantity of flower like structure of pure ZnO and 1 wt. % Pd doped ZnO. Each flower consists of small hexagonal prism like structure of ZnO. Fig. 2 (c) and (d) shows FE - SEM images for 3 wt. % of Pd doped ZnO and 6 wt. % Pd doped ZnO. It is observed that both consist of hexagonal prism-like structure of ZnO crystalline phase. Fig. 2 (e) shows the high resolution image of 3 wt.% Pd doped ZnO shows that the height and width of the prism ranges from 400 nm to 1 μ m from these results it can be concluded that there is incorporation of Pd in ZnO.



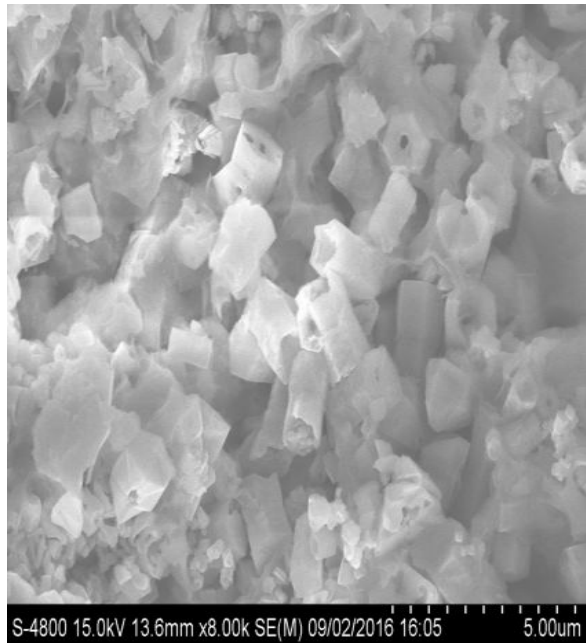
(a)



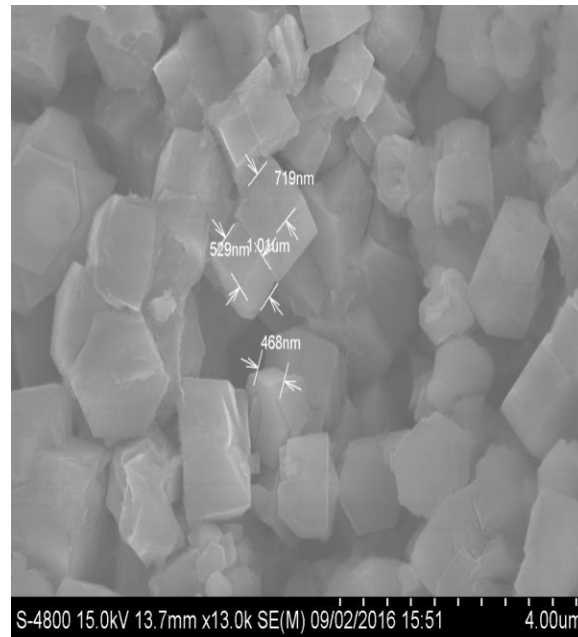
(b)



(c)



(d)

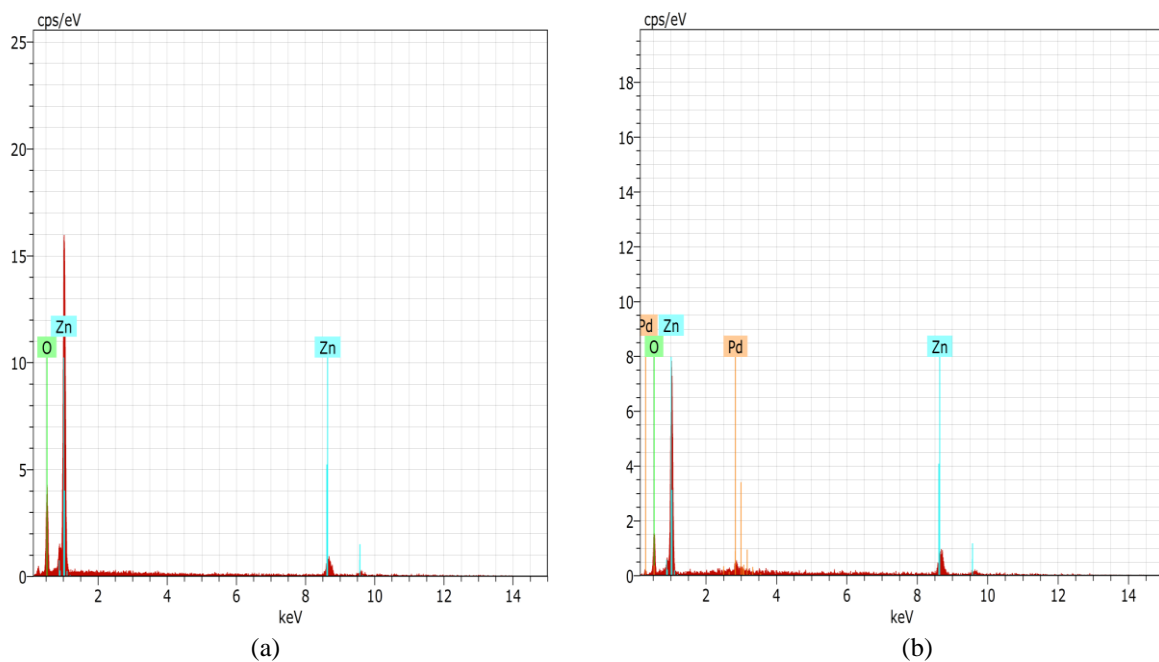


(e)

Figure 3: FESEM images of (a) Pure ZnO, (b) 1wt.% Pd doped ZnO, (c) 3 wt.% Pd doped ZnO, (d) 6 wt. % Pd doped ZnO and (e) high resolution image of 3 wt.% Pd doped ZnO.

3.1.3 Energy dispersive X-ray analysis (EDAX):

The elemental analysis of pure and Pd doped ZnO thick films were carried out using EDAX (JOEL, JED-2300, Germany). Fig. 4 shows EDAX pattern of (a) Pure ZnO, (b) 1wt.% Pd doped ZnO, (c) 3 wt.% Pd doped ZnO, (d) 6 wt. % Pd doped ZnO. The EDAX analysis shows presence of only Zn, Pd and O as expected, no other impurity elements were present in the Pd doped ZnO. The EDAX result shows variation in Zn/O ratio with variation in doping concentration.



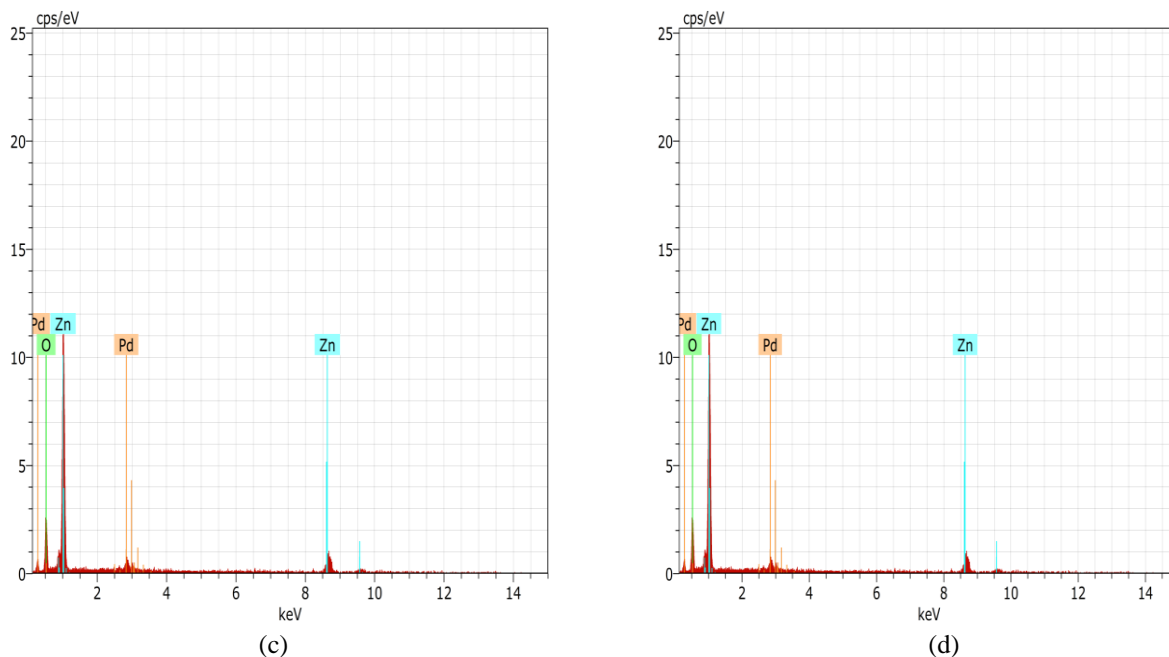


Figure 4: EDAX spectrum of (a) Pure ZnO, (b) 1wt.% Pd doped ZnO, (c) 3 wt.% Pd doped ZnO, (d) 6 wt. % Pd doped ZnO.

3.2. Gas sensing Characteristics:

3.2.1 I-V characteristics:

Fig.5 shows the I-V characteristics of the Pure and Pd doped ZnO thick films. Keithley 6487 picoammeter cum voltage source was used for measurement. The bias voltage was increased from 0 to 25 volts and the corresponding current was noted. The voltage was increased in steps of 5 volts. The same process was performed for negative voltage. It is observed from I-V characteristics that the curves for pure and Pd doped ZnO thick films shows symmetry indicate the contacts between the films and the probes of the system are ohmic in nature [26].

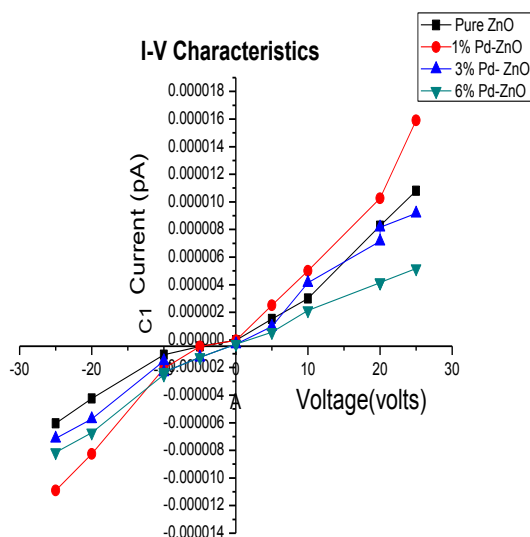


Figure 5: I-V characteristics of pure and Pd doped ZnO thick films.

3.2.2 Electrical conductivity:

Fig. 6 gives graphical representation of variation of log (conductivity) with operating temperature of pure and Pd doped ZnO thick films. From the graph the nature of thick films are semiconducting nature. The

increase in conductivity with increasing temperature could be attributed to negative temperature coefficient and semiconducting nature of pure and all Pd doped ZnO thick films.

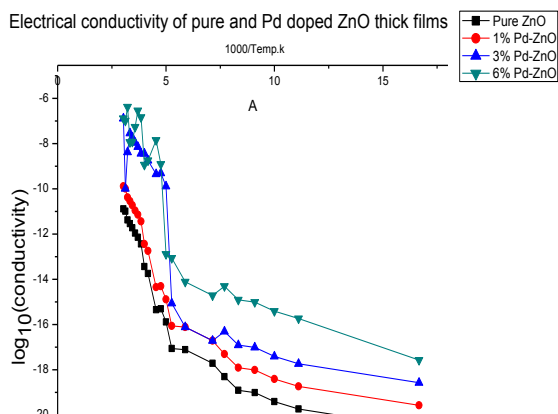
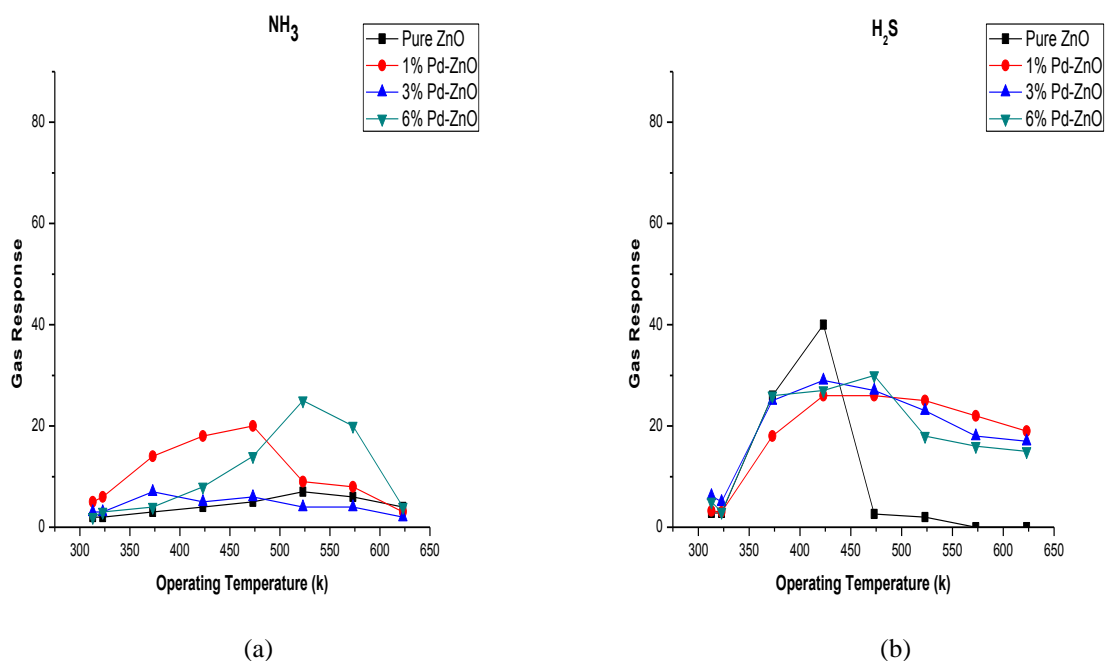


Figure 6: Conductivity temperature profile of pure ZnO and Pd doped ZnO thick films.

3.3 Gas response:

The gas sensing behavior of Pd doped ZnO thick was studied by using static gas measurement system. The DC resistance of pure and Pd doped ZnO thick films were measured by using half bridge method as a function of temperature in air as well as in NH_3 , H_2S , CO_2 , LPG and Ethanol vapour in gas atmosphere. The operating temperature was varied at the interval of 50 °K. From the measured resistance in air as well as in gas atmosphere, the sensitivity of gas was determined at particular operating temperature.

The gas sensing properties of pure and 1 wt. %, 3 wt. %, and 6 wt. % Pd doped ZnO thick films have been studied. On the basis of measured data, the sensitivity, selectivity, response and recovery time of thick film sensor for a fixed gas concentration of 1000 ppm in air ambient condition was calculated. Also the response of gas with variation of gas concentration at optimum operating temperature is studied.



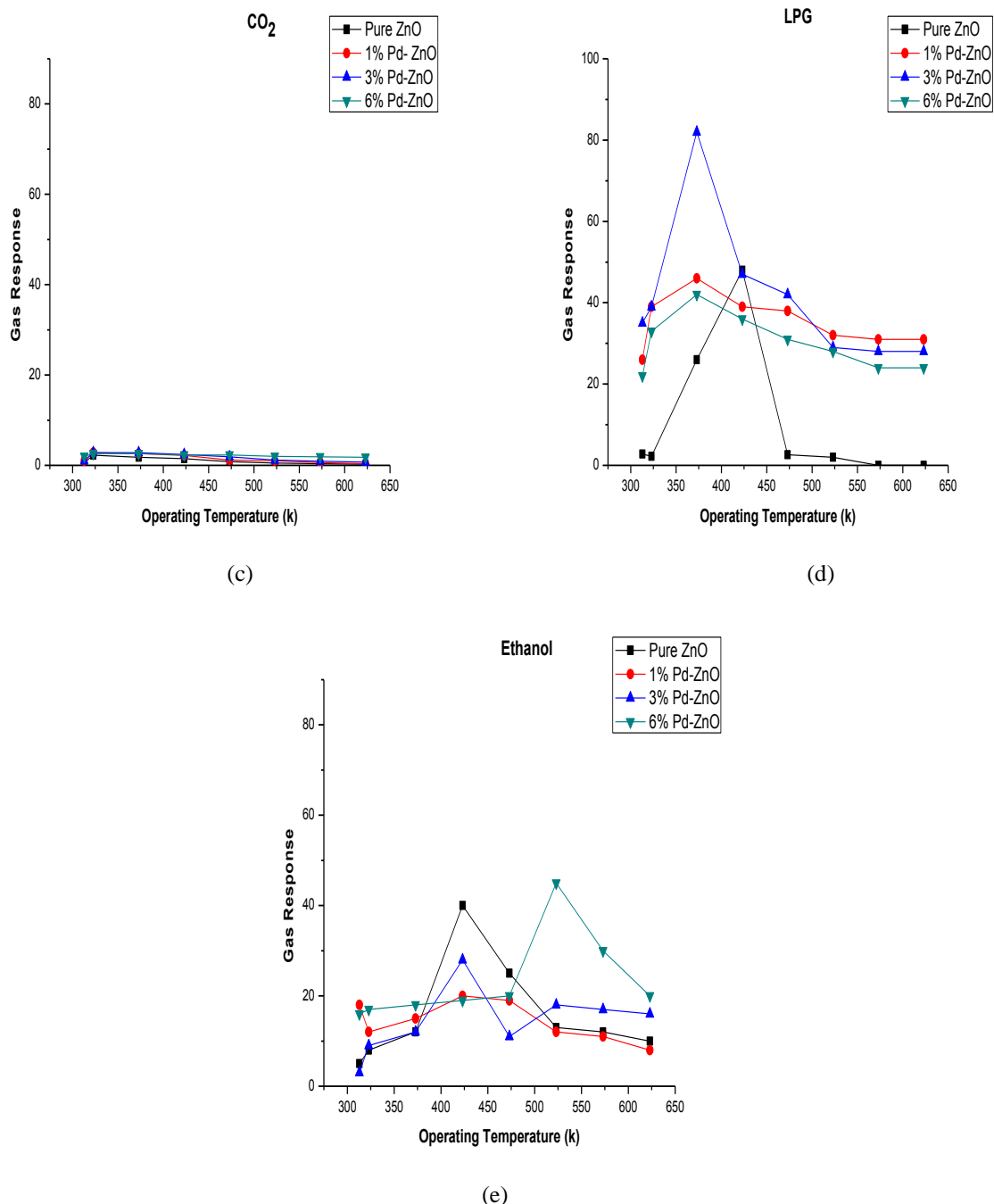


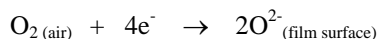
Figure 7(a – e): Variation of gas response of pure and Pd doped ZnO thick films with operating temperature for NH₃, H₂S, CO₂, LPG and Ethanol gas.

The gas response for pure and Pd doped ZnO thick films was noted from room temperature to 623 °K for 1000 ppm of different gases i.e. NH₃, H₂S, CO₂, LPG and Ethanol vapour. From figure 7 (a-e), it is observed that Pd doped ZnO thick films are sensitive to LPG at room temperature than other tested gases i.e. NH₃, H₂S, CO₂ and Ethanol vapour. The 3 wt. % Pd doped ZnO thick films show higher sensitivity to LPG than other doping concentrations. This film has shown sensing response to LPG i.e. 32 at room temperature and higher sensing response i.e. 82 at operating temperature 350 °K. The composition of LPG is as follows:

TABLE 1: Composition of LPG gas.

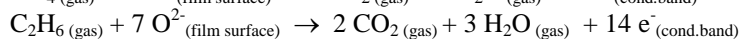
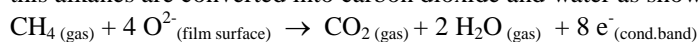
Composition of LPG in volume percentage	CH ₄	C ₂ H ₆	C ₃ H ₈	C ₄ H ₈	C ₄ H ₁₀	C ₅ H ₁₂
	6	8	11.5	15	55	4.5

As butane is an important element of LPG, to dissociate butane into lower alkanes, there is need of higher temperature. As the Van der Waals forces are very strong, carbon-hydrogen and carbon - carbon bonds are also strong. These carbon-hydrogen and carbon - carbon bonds requires very high temperature to breakdown the bonds. When these bonds are broken, there is separation of hydrogen and carbon. Then adsorption of atmospheric oxygen O₂ on the surface of the film takes place and acquires the electron from conduction band as follows:

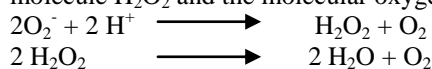


As a result of this, there is decrease in conductivity of the thick film.

When there is reaction between oxygen and alkanes, number of reactions takes place and as a result of this alkanes are converted into carbon dioxide and water as shown in the following reactions:



This indicates that the mechanism is of n-type. The molecular oxygen O₂ is converted into O₂⁻ when the temperature is high. Also in the reaction, hydrogen ions H⁺ are produced due to decomposition of alkanes. Then there is a reaction between the O₂⁻ anion super-oxide and H⁺ hydrogen ions which leads to formation of water molecule H₂O₂ and the molecular oxygen O₂ [27-30]. This reaction is as shown below:



When Pd doped ZnO thick film sensor element exposed to LPG, it decomposes into carbon and hydrogen species. These carbon and hydrogen species then reacts with adsorbed oxygen. This results in the release of electron in the conduction band which then improves the catalytic activity of surface of thick film. The rate of reaction between adsorbed species as well as rate of adsorption depends on the temperature. In case of semiconductors, a maximum is obtained at certain temperature in the curves of gas response versus operating temperature. This maximum temperature is used as the working temperature of sensor. As there is change in temperature, there is also the change in the form of the adsorbed oxygen. Hence, coverage of adsorbed oxygen as a function of temperature also affects the observed shape of gas response curve. Hence by adding the impurities which adsorbs or reacts with the target gas, the selectivity can be enhanced. In Pd doped ZnO thick films, the number of grains of ZnO and Pd are linked with each other through the grain boundaries. As a result of this, barrier height among the grains is formed. Due to the formation of these barrier height in the grains, in absence of the target gas there is increase in the resistance.

3.4 Selectivity :

Selectivity is defined as the ability of a sensor to respond to certain gas in the presence of other gases. Selectivity of one gas over others is defined as the maximum response of sensor element in presence of other gas to the maximum response sensor element in presence of target gas at optimum operating temperature. Fig. 8 shows gas response of 3 wt. % Pd doped ZnO thick film for different gases and it is found that 3 wt. % Pd doped ZnO thick films shows maximum gas response for LPG over other gases.

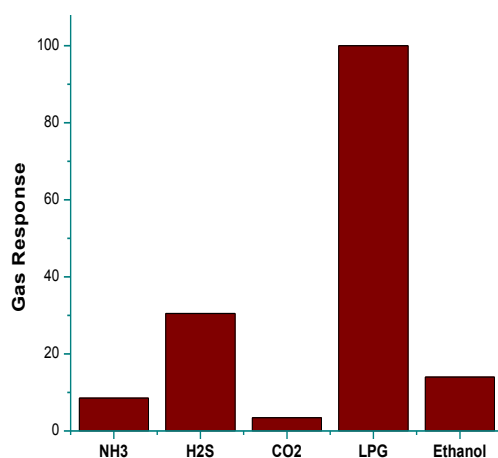


Figure 8: Gas response of 3 wt.% Pd doped ZnO thick film.

3.5 Response and recovery time of thick film sensor:

In practical applications, response and recovery time for the particular gas are important factors. The response and recovery time of sensors is the time reaching 90% of final stable values [30]. Fig. 9 illustrates response and recovery time of 3% Pd-doped ZnO thick film sensors. The response time and recovery time of the sensor was (8 s) and (16 s) respectively to LPG. The quick response of sensor element to LPG may be due to faster oxidation of gases.

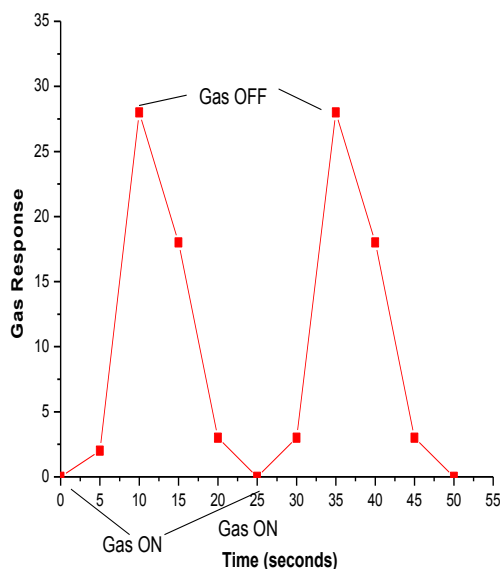


Figure 9: Gas response of 3 wt. % Pd doped ZnO thick film sensor towards LPG with time.

IV. Conclusions

Zinc oxide and Palladium doped zinc oxide nanoparticles were successfully synthesized without using surfactant by microwave assisted precipitation method. The response of pure ZnO thick film toward LPG was very poor than the response of Pd doped ZnO thick films. Pd doped ZnO thick films show sensing response to LPG at room temperature. The 3 wt. % Pd doped ZnO thick films show sensitivity to LPG at room temperature and maximum sensitivity at 350 °K temperature with fast response time (8 s) and recovery time (16 s). Hence Pd doping in ZnO is an appropriate dopant to enhance sensitivity and selectivity of sensor element toward LPG. The 3 wt. % Pd doped ZnO thick film sensors found to be sensitive and selective to LPG at operating temperature hence it is use as sensing material for LPG sensor element.

References

- [1]. P. Mitra, A. P. Chatterjee and H.S. Maiti, ZnO thin film sensor, *Materials Letters*, 35 (1998) 33-38.
- [2]. A. P. Chatterjee, P. Mitra and A. K. Mukhopadhyay, Chemically deposited zinc oxide thin film gas sensor, *Journal of Materials Science*, 34, 1999, 4225–4231.
- [3]. H.T. Wang, B.S. Kang, F. Ren, L.C. Tien, P.W. Sadik, D.P. Norton, S.J. Pearton and J. Lin, Hydrogen-selective sensing at room temperature with ZnO nanorods, *Applied Physics Letters*, 86 (24), 2005, 243503.
- [4]. L. C. Tien, P. W. Sadik, D. P. Norton, L. F. Voss, S. J. Pearton, H. T. Wang, B. S. Kang and F. Ren, Hydrogen sensing at room temperature with Pt-coated ZnO thin films and nanorods, *Applied Physics letters*, 87, 2005, 222106.
- [5]. S. Verhelst and R. Sierens, Hydrogen engine-specific properties, *International Journal of Hydrogen Energy* 26 (9), 2001, 987–990.
- [6]. X. Bévenot, A. Trouillet, C. Veillas, H. Gagnaire and M. Clément, Hydrogen leak detection using an optical fibre sensor for aerospace applications, *Sensors and Actuators B*, 67, 2000, 57–67.
- [7]. Q. Wan, Q. H. Li, Y. J. Chen, T. H. Wang, X. L. He, J. P. Li and C. L. Lin. Fabrication and ethanol sensing characteristics of ZnO nanowire gas sensors, *Applied Physics letters*, 84, 2004, 3654–3656.
- [8]. I. Yonenaga, Thermo-mechanical stability of wide-bandgap semiconductors: high temperature hardness of SiC, AlN, GaN, ZnO and ZnSe, *Physica B*, 308, 2001, 1150–1152.
- [9]. M. Kashif, S.M. Usman Ali, M. E. Ali, H.I. Abdulfafour, U. Hashim, M. Willander and Z. Hassan, Morphological, optical and Raman characteristics of ZnO nanoflakes prepared via a sol–gel method, *Physica Status Solidi A*, 209 (1), 2012, 143–147.
- [10]. S. M. Usman Ali, N. H. Alvi, Z. Ibupoto, O. Nur, M. Willander and B. Danielsson, Selective potentiometric determination of uric acid with uricase immobilized on ZnO nanowires, *Sensors and Actuators B: Chemical*, 152 (2), 2011, 241–247.
- [11]. M. M. Arifat, B. Dinan, S. A. Akbar and M. A. Haseeb, Gas sensors based on one dimensional nanostructured metal-oxides: a review, *Sensors*, 12 (6), 2012, 7207–7258.
- [12]. H.T. Wang, B.S. Kang, F. Ren, L.C. Tien, P.W. Sadik, D.P. Norton, S.J. Pearton and J. Lin, Detection of hydrogen at room temperature with catalyst-coated multiple ZnO nanorods, *Applied Physics A*, 81 (6), 2005, 1117–1119.

- [13]. Z. Liu, L. Junwei, Y. Jing, X. Ying, J. Zhengguo, Mechanism and characteristics of porous ZnO films by sol-gel method with PEG template, *Materials Letters*, 62, 2008, 1190-1193.
- [14]. P. Pawinrat, O. Mekasuwandumrong and J. Panpranot, Synthesis of Au-ZnO and Pt-ZnO nanocomposites by one-step flame spray pyrolysis and its application for photocatalytic degradation of dyes, *Catalysis Communications*, 10 (10), 2009, 1380-1385.
- [15]. H. Zeng, W. Cai, P. Liu, X. Xu, H. Zhou and C. Klingshirn, ZnO-Based Hollow Nanoparticles by Selective Etching: Elimination and Reconstruction of Metal-Semiconductor Interface, Improvement of Blue Emission and Photocatalysis, *ACS Nano*, 2, 2008, 1661-1670.
- [16]. R. Georgekutty, M. K. Seery and S. C. Pillai, A Highly Efficient Ag-ZnO Photocatalyst: Synthesis, Properties, and Mechanism, *Journal of Physical Chemistry C*, 112, 2008, 13563-13570.
- [17]. I. Hayakawa, Y. Iwamoto, K. Kikuta and S. Hirano, Gas sensing properties of platinum dispersed-TiO₂ thin film derived from precursor, *Sensors and Actuators B: Chemical*, 62, 2000, 55-60.
- [18]. O. Lupan, G. Chai and L. Chow, Novel hydrogen gas sensor based on single ZnO nanorod, *Microelectronic Engineering*, 85 (11), 2008, 2220-2225.
- [19]. O. García-Serrano, O. Goiz, F. Chavez, G. Romero-Paredes and R. Peña-Sierra, Pd-decorated ZnO and WO₃nanowires for sensing applications, *IEEE Sensors*, 2011, 998-1001.
- [20]. S. J. Jung and H. Yanagida, The characterization of CuO/ZnO heterocontact type gas sensor having selectivity for CO gas, *Sensors and Actuators B*, 37, 1996, 55-60.
- [21]. S. Fardindoost, A. Irajizad, F. Rahimi and R. Ghasempour, Pd doped WO₃ films prepared by sol-gel process for hydrogen sensing, *International Journal of Hydrogen Energy* 35 (2), 2010, 854-860.
- [22]. R. B. Pedhekar and F. C. Raghuvanshi, CeO₂ activated ZnO-TiO₂ thick film for CO₂ gas sensor, *International Journal of Engineering, Science Invention*. 6(8), 2017, 20-28.
- [23]. S. Ren, G. Fan, S. Qu and Q. Wang, Enhanced sensitivity at room temperature of ZnO nanowires functionalized by Pd nanoparticles, *Journal of Applied Physics*, 110 (8), 2011, 084312-084316.
- [24]. B. L. Zhu, C.S. Xie, W. Y. Wang, K. J. Huang and J. H. Hu, Improvement in gas sensitivity of ZnO thick film to volatile organic compounds (VOCs) by adding TiO₂, *Materials Letters*, 58(5), 2004, 624-629.
- [25]. M. Kashif, M.E.Ali, Syed M. Usman Ali and U. Hashim, Sol-gel synthesis of Pd doped ZnO nanorods for room temperature hydrogen sensing applications, *Ceramics International*, 39(6), 2013, 6461-6466.
- [26]. Joint Committee on powder Diffraction Standards (JCPDS), Inorganic Volume, 1980, Swarthmore, PA, Card No. 6-620.
- [27]. R. B. Pedhekar, F. C. Raghuvanshi and V. D. Kapse, Liquid Petroleum Gas Sensing Performance Enhanced by CuO Modification of Nanocrystalline ZnO-TiO₂, *Materials Science – Poland*. 34(3), 2016, 571-581.
- [28]. D. R. Patil and L. A. Patil, Room temperature chlorine gas sensing using surface modified ZnO thick film resistors, *Sensors and Actuators B: Chemical*, 1, 2007, 546-553.
- [29]. Z. Tianshu, Z. Ruifang, S. Yusheng and L. Xingqin, Influence of Sb/Fe ratio and heating temperature on microstructure and gas-sensing property of Sb₂O₃-Fe₂O₃ complex oxide semiconductors, *Sensors and Actuators B*, 32, 1996, 185-189.
- [30]. R. B. Pedhekar, F. C. Raghuvanshi and V. D. Kapse, Low Temperature H₂S Gas Sensor Based on Fe₂O₃ Modified ZnO-TiO₂ Thick Film, *International Journal of Materials Science and Engineering*. 3, 2015, 219-230.

Yogita Patil, R. B. Pedhekar, F. C. Raghuvanshi, "Palladium-Doped Zinc Oxide Nanomaterial For Liquefied Petroleum Gas Detection " *International Journal of Engineering Science Invention (IJESI)*, Vol. 09(01), 2020, PP 32-42